High-Resolution Absorption Studies of the $\tilde{A}^1A_2-\tilde{X}^1A_1$ $2_0^2 4_0^1$ Band of Formaldehyde

Martin B. Crow, Alex Gilchrist, Gus Hancock, Rob Peverall, Graham Richmond, Grant A. D. Ritchie,* and Sarah R. Taylor

Department of Chemistry, Physical and Theoretical Chemistry Laboratory, University of Oxford, South Parks Road, Oxford, OX1 3QZ, U.K.

Received: March 16, 2009; Revised Manuscript Received: April 27, 2009

Absolute peak absorption cross sections and pressure broadening coefficients have been recorded with sub-Doppler limited instrumental resolution for selected rotational lines in the $2_0^2 4_0^1$ vibronic band of the formaldehyde $\tilde{A}^1A_2-\tilde{X}^1A_1$ electronic transition. The measured absorption cross sections range between (0.18 ± 0.01) and $(10.1 \pm 0.08) \times 10^{-19}$ cm^2 molecule^{-1} and are considerably larger than values from the literature recorded using apparatus where instrumental broadening was significant. However, comparisons with spectral simulations with equivalent resolution from Smith et al. (*J. Phys. Chem. A* **2006**, *110*, 11645−11653) are in excellent agreement. Pressure broadening was studied for the collision partners CH_2O, CO_2, N_2, O_2, Ne, Kr, Ar, and He, and the resulting broadening coefficients were found to be reduced in comparison to equivalent values measured in infrared regions, consistent with the reduced dipole moment of the upper state probed in this work. Cavity-enhanced absorption spectroscopy (CEAS) measurements were undertaken using calibrated low concentration (2.9−4.6 ppmv) samples from a permeation source and demonstrate a noise equivalent absorption of 1.2×10^{-6} cm^{-1} Hz$^{-1/2}$. This implies a minimum detectable formaldehyde concentration with the current system in atmospheric air of 172 ppbv Hz$^{-1/2}$.

Introduction

The simplest aldehyde compound, formaldehyde, is an important constituent of the oxidation chemistry of the troposphere. Produced by the oxidation of hydrocarbons such as methane, its photochemical activity is an important source of radical species such as HCO, H, and subsequently HO_2 as well as molecular hydrogen and carbon monoxide. At ground level, formaldehyde is a toxic industrial pollutant, and suspected carcinogen. Concentrations in urban environments are typically a few tens of ppbv,[1−3] while the background concentration in unpolluted air is of the order of 100 pptv.[4,5]

The spectroscopy and photochemistry of formaldehyde have been reviewed in detail by Moule and Walsh,[6] and Clouthier and Ramsay.[7] Formaldehyde is photochemically active in the troposphere within the electronic $\tilde{A}^1A_2-\tilde{X}^1A_1$ band system, which is primarily formed from a progression of the CO stretching vibration (ν_2), in combination with excitation of either one or three quanta in the out of plane ν_4 bending vibration. Weaker bands involving the ν_4 and ν_5 modes in isolation, and a combination of the ν_4 and ν_6 modes are also featured. The $\tilde{A}-\tilde{X}$ system is a symmetry-forbidden transition and is thus relatively weak for an electronic transition, with integrated band intensities typically of order 10^{-17} cm^2 molecule^{-1} cm^{-1}. This is similar in magnitude to fundamental vibrational transitions in the mid-infrared region,[8] and larger than other conveniently located rovibrational transitions in the near-infrared region.[9]

Recent spectroscopic investigations of formaldehyde in the $\tilde{A}-\tilde{X}$ band system have focused primarily on the measurement of absolute absorption cross sections and their temperature and/or pressure dependence. Cantrell et al.[10] measured absorption cross sections using an interferometer-based spectrometer over the wavelength range 300−360 nm, with temperatures ranging between 223 and 293 K and a resolution of 1 cm^{-1}. They studied the temperature dependence of integrated band intensities and found temperature gradients at selected wavelengths to be around 0.3% of their measured cross sections. They also noted that nonlinear absorption occurred in regions of the spectrum containing strongly absorbing features. Meller and Moortgat[11] then extended this range to cover 225−375 nm, again measuring cross sections and temperature gradients with a resolution of 2.73 cm^{-1}.

More recently, Pope et al.[12] and Smith et al.[13] measured absorption cross sections across the range 300−340 nm at a resolution estimated to be 0.35 cm^{-1}. By fitting spectral simulations to their data, they also provided optimized values for the upper state spectroscopic parameters and calculated transition dipole moments for each of the vibronic bands that they probed. At longer wavelengths, Co et al.[14] probed the $2_0^0 4_0^1$ vibronic band using a high-resolution Fourier transform spectrometer with a resolution of 0.027 cm^{-1}. These were the first measurements to be performed in the UV region with an instrumental bandwidth smaller than the thermal Doppler width of formaldehyde, by a factor of around 2 in this case. Gratien et al.[8,15] have performed a comparison of formaldehyde integrated absorption cross sections in the infrared and ultraviolet regions by recording spectra between 300 and 360 nm with a resolution of 16 cm^{-1} simultaneously with spectra in the ranges 1660−1820 and 2600−3100 cm^{-1} with 0.1 cm^{-1} resolution.

In recent years, the use of compact, affordable narrow bandwidth diode lasers has become increasingly common in molecular spectroscopy. These lasers typically operate in the near-IR or visible regions and thus can be used to probe vibrational overtone transitions of small molecules, with instrumental resolution a small fraction of the Doppler width. We have constructed an absorption spectrometer in the ultraviolet region, with the aim to use sum-frequency generation with narrow-band continuous wave lasers to probe stronger electronic

* Corresponding author. E-mail: Grant.Ritchie@chem.ox.ac.uk. Phone: +44 (0)1865 285723. Fax: +44 (0)1865 275 410.

10.1021/jp9023475 CCC: $40.75
Published on Web 05/21/2009

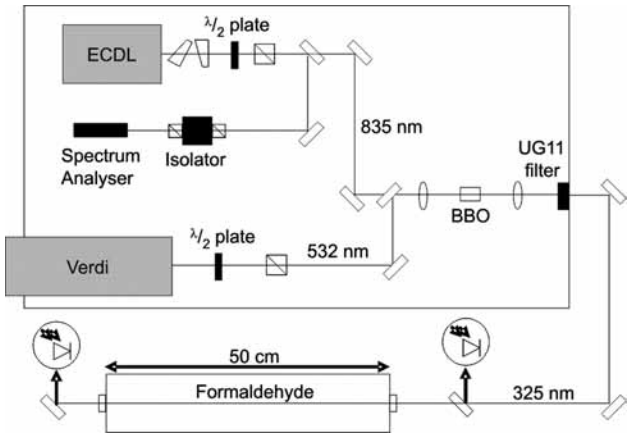

Figure 1. Schematic of the sum frequency generation setup used to produce tunable, narrow band radiation around 325 nm by mixing radiation from an external cavity diode laser (labeled ECDL) with that of a diode pumped solid state laser (labeled Verdi) in a type I β-BBO crystal. In the cavity-enhanced absorption experiments a pair of high reflectivity cavity mirrors are placed in the cell and the detection photodiode replaced by a photomultiplier tube.

transitions. To our knowledge the only other study of formaldehyde with similar resolution is that of Motsch et al.,[16] who used a frequency-doubled ring dye laser to record absorption spectra of two vibronic bands in the $\tilde{A}-\tilde{X}$ transition, and fitted spectral simulations to their data to provide a set of upper state spectroscopic constants that compared well with those of Smith et al.[13]

We report measurements of the absolute absorption cross sections and pressure broadening coefficients of several rotational lines in the $\tilde{A}-\tilde{X}$ $2_0^2 4_0^1$ vibronic band with insignificant contributions from instrumental broadening. Measurement of pressure broadening parameters can provide chemically interesting information on the intermolecular forces acting between the probed species and chosen collision partners. At a more practical level, accurate knowledge of absorption cross sections and pressure broadening processes greatly benefits the prediction of absorption spectra for the purpose of atmospheric monitoring. In addition, we demonstrate the use of this high-resolution ultraviolet source in an optical cavity enhancement methodology to explore the potential for its use in atmospheric monitoring.

Experimental Methods

The experiments were carried out with a custom-built spectrometer, consisting of a narrow band, tunable continuous wave ultraviolet (UV) laser source, and an absorption cell, to which formaldehyde vapor was added along with a buffer gas, if desired. The UV source produced radiation around 326 nm by sum frequency mixing of a high-power, fixed frequency laser operating in the visible region with a tunable diode laser operating in the near-infrared. A schematic diagram of the setup is shown in Figure 1. The first laser is a diode pumped Nd:YVO_4 laser (Coherent Verdi V5), generating 532 nm light at power levels up to 5 W, with a specified bandwidth of 5 MHz. The beam was passed through a zero-order half-waveplate and polarizer (Thorlabs WPH05M-532 and GL5-A), and directed through a plano-convex lens (UQG, 10 cm focal length) by dichroic mirrors (Laseroptik, HR 532 nm). A temperature controlled β-BBO crystal (Casix, type I, $\theta_m = 35.8°$) was placed at the focal point and mounted on a precision rotation stage (Thorlabs PR01/M), which was in turn attached to an $x-y-z$ translation stage (Thorlabs PT3/M).

The second laser is an external cavity diode laser (Sacher Lasertechnik, TEC-500), tunable around 841 nm, with an output power of ~40 mW and a quoted bandwidth of less than 1 MHz. The diode laser was first passed through a pair of anamorphic prisms, which reshaped the initially elliptical beam profile to closely match that of the Nd:YVO_4 laser. A waveplate and polarizer (B.Halle) were again used to set the polarization, before the beam was overlapped with the visible beam through the focusing lens and β-BBO crystal. The diode laser frequency was varied by angle tuning the grating in its external cavity (Littrow configuration) during experiments. A wavemeter (Coherent Wavemaster) was used to measure the wavelength of the laser when coarse tuning to chosen regions of the formaldehyde spectrum. During experiments, a partial reflection of the beam was passed through an optical isolator (Isowave I-7090-CM), and aligned into a spectrum analyzer (Melles-Griot, 10 GHz free spectral range), to allow calibration of the relative frequency scale.

Ultraviolet radiation was produced by angle tuning the β-BBO crystal in the plane of its optical axis in order to achieve phase matching. Typical output power levels were in the range 2−4 μW, depending on the intensity levels of the two input beams, corresponding to an efficiency of 57% of the theoretical maximum, as predicted according to Boyd and Kleinman.[17] The resulting UV radiation was then collimated by a second lens (UQG, 10 cm focal length) and separated from the visible/near-infrared beams using a UG11 optical filter, before being directed through the absorption cell by a pair of dichroic mirrors (Laseroptik, HR 280−400 nm) onto an amplified photodiode detector (Thorlabs PDA25K-EC). The second of these mirrors was attached to a flip mount, which allowed the beam to be directed onto an identical detector placed before the cell for background measurements. For cavity-enhanced absorption spectroscopy (CEAS) experiments, the photodiode after the cell was replaced by a photomultiplier tube (Electron Tubes 9125 QB) terminated by a 1 MΩ impedance, due to the low intensity of light transmitted through the cavity. Frequency tuning of the UV radiation, typically over a range of around 40 GHz, was achieved by application of a voltage ramp from a signal generator (Thurlby Thandar Instruments TG230) to the piezoelectric driver of the diode laser. Signals from both detectors, along with the etalon trace from the spectrum analyzer were acquired using a digital storage oscilloscope (Tektronix TDS380), and transferred to a computer via a GPIB interface using custom-written software in Labview for analysis.

The absorption cell was constructed from stainless steel and was 50 cm in length. Its design accommodated the installation of optical components, such as cavity mirrors (LayerTec GmbH), for use in the CEAS experiments. In the cavity experiments, we found that fine adjustment of the alignment of the cavity, together with mechanical vibrations from the vacuum pumps, were sufficient to reduce the mode structure of the cavity and provide a smooth baseline during experiments. Pressure measurements were made using calibrated capacitance manometers (Leybold Ceravac, 0−10 Torr and 0−1000 Torr), and the cell evacuated using a turbomolecular pump, backed by a rotary vane pump (Leybold Turbovac 50 and Trivac D16B).

For direct absorption measurements monomeric formaldehyde was prepared by the cracking of paraformaldehyde, as described by Spence and Wild.[18] Formaldehyde vapor was passed through a dry ice/acetone trap for purification and stored in a liquid nitrogen trap. FTIR spectra of the formaldehyde samples produced by this method were periodically recorded and showed no evidence of impurities such as water, or potential decomposi-

tion products, for example, acetone and acetaldehyde. Comparison with integrated band intensities from the literature[8] suggested that the typical purity of the formaldehyde produced by this method ranged between 92% and 96%. It is likely that a component of the reduction from 100% measured purity is due to loss by dimerization or wall adsorption of the relatively high pressure (~3−5 Torr) formaldehyde samples on the time scale of the FTIR measurements. The time scale of the lower pressure UV absorption experiments was typically around 30 min, and we observed no measurable loss of formaldehyde over this time period due to photolysis by the UV source or removal from the gas phase.

The cracking apparatus was connected directly to the absorption cell by PTFE tubing and was used to fill the cell with static samples of formaldehyde vapor. The buffer gases used, as described in the results section, were CO_2 (BOC, 99.995%), N_2 (BOC, 99.998%), O_2 (BOC 99.999%), Kr (BOC 99.999%), Ar (BOC 99.999%), Ne (BOC 99.994%), and He (BOC 99.999%). In the cavity-enhanced absorption experiments, a permeation tube (Kin-Tek) was used to provide calibrated, low concentration samples of formaldehyde. The tube was maintained at a constant temperature of 80 °C, resulting in emission of formaldehyde vapor at a specified rate of 649 ± 13 ng min^{-1}. A buffer gas, such as N_2, was passed through a calibrated mass-flow controller (Tylan FC 026) at a known flow rate and over the permeation tube. This resulted in a mixture of specified formaldehyde concentration (typically ~3 ppmv), diluted in N_2, which was flowed through the absorption cell at a chosen total pressure (typically 100 Torr). The formaldehyde concentration of the mixture was varied by adjustment of the buffer gas flow rate across the permeation tube.

Results and Discussion

We have applied our spectrometer to the absorption spectroscopy of formaldehyde vapor in its $\tilde{A}-\tilde{X}$ $2_0^2 4_0^1$ vibronic band. The bandwidth of the UV source is limited by the combined bandwidths of the two input beams and would thus be expected to be less than 10 MHz, or 3.3×10^{-4} cm^{-1}. This is approximately 2 orders of magnitude narrower than the room temperature thermal Doppler width of formaldehyde lines in the $\tilde{A}-\tilde{X}$ transition and around 3 orders of magnitude narrower than that achieved with apparatus previously used to measure absorption cross sections of formaldehyde in this region.[10−13,15]

We have recorded two contiguous absorption spectra, as shown in Figures 2 and 3 spanning ~8−10 cm^{-1} sections of the $\tilde{A}-\tilde{X}$ $2_0^2 4_0^1$ vibronic band at pressures of 450 and 700 mTorr, respectively. Pane (a) in each case shows our measured absorption spectra, where the intensity is plotted as the base e absorbance according to the Beer−Lambert law, given by eq 1 where $I_0(\nu)$ is the laser intensity measured on the photodiode

$$-\ln \frac{I(\nu)}{I_0(\nu)} = \sigma(\nu)cl \qquad (1)$$

placed before the formaldehyde sample, $I(\nu)$ is the intensity measured after the sample, $\sigma(\nu)$ is the absorption cross section, c is the concentration of formaldehyde, and l is the path length containing the sample.

Pane (b) in each figure shows a spectral simulation of the corresponding region, calculated in PGopher using input parameters supplied in the Supporting Information of Smith et al.[13] These parameters include rotational and centrifugal distortion constants for the ground and excited electronic states,[7]

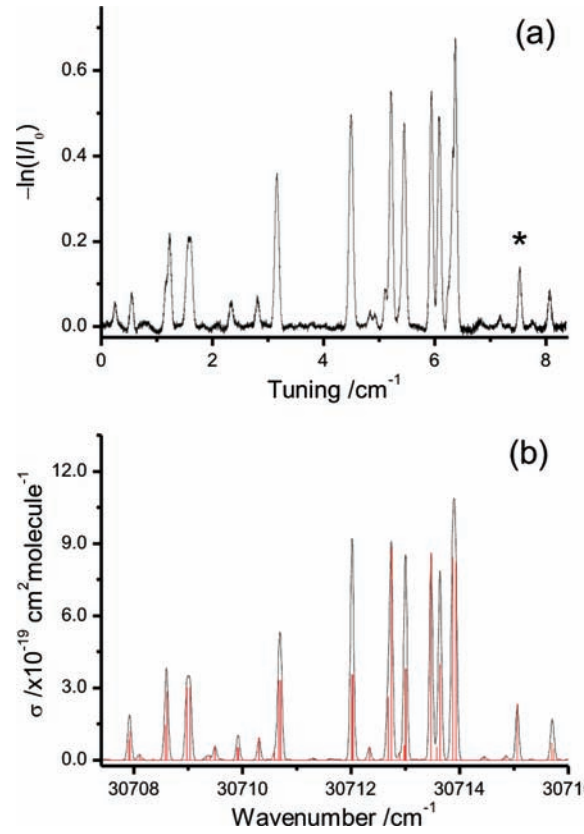

Figure 2. Absorption spectrum of a section of the formaldehyde $\tilde{A}-\tilde{X}$ $2_0^2 4_0^1$ vibronic band, acquired with 450 mTorr formaldehyde. Panel (a) shows the measured data while (b) shows a spectral simulation of the corresponding region, where red lines indicate line positions and relative intensities and the black line is a prediction of the spectrum with Doppler line widths. The asterisk highlights a single rotational line used for pressure broadening/absorption cross-section measurements as described in the text.

where the excited state constants have previously been refined by Smith et al.,[13] who fitted spectral simulations to their data acquired across the range 300−340 nm. We have not carried out any further optimization of the molecular constants and have only changed the resolution function to a Gaussian profile with the expected thermal Doppler width of formaldehyde at the ambient temperature of the laboratory. We find generally excellent agreement between our measured absorption spectra and the simulations, as shown in the figures. It is interesting to note that perturbations occur between certain upper state levels probed in the $2_0^2 4_0^1$ band and levels in the nearby $^3A_2$ state, as studied by Brand and Stevens[20] and Birss et al.[21] They found 29 lines and around 40 upper state levels that were perturbed, through measurements of magnetic rotation. Of the lines found by Brand and Stevens, one appears in Figure 2 at ~30709 cm^{-1}, assigned in the PGopher simulation[13,19] as the overlapping pair $^rR_{9,3}(11)$ and $^rR_{8,3}(11)$, with the notation $^{\Delta K_a}\Delta N_{K_c K_a}(J)$, nevertheless Figure 2 shows good agreement between data and simulation relative to the surrounding features. On closer inspection of Figure 3 however, it appears that some of the deviation between our data and the simulations may be due to such perturbations. Two of the upper rotational states found by Birss et al. to be perturbed by the triplet state are (in the notation J_{K_c,K_a}) $20_{4,17}$ and $11_{9,2}$. Weak lines probing these states appear in the simulation at 30634.52 cm^{-1} and 30636.83 cm^{-1}, respectively, and show relatively poor agreement with our data compared to the surrounding features.

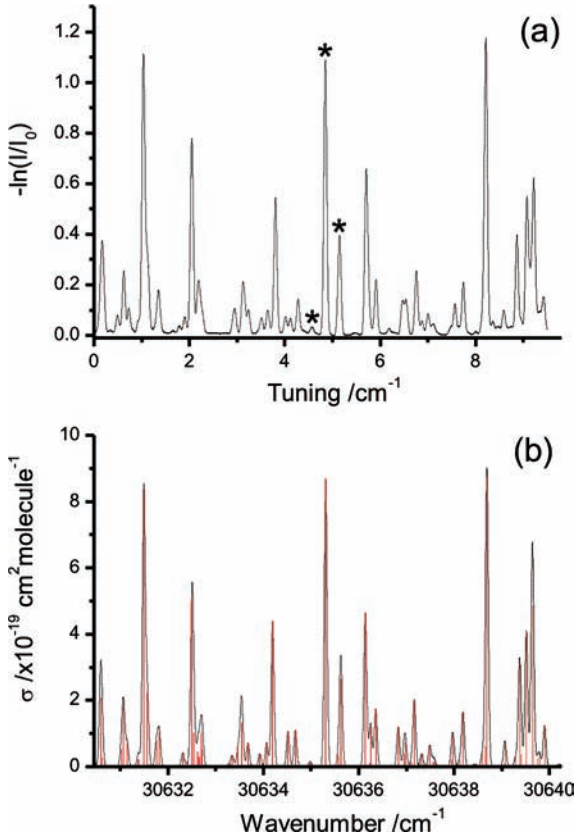

Figure 3. Absorption spectrum of a section of the formaldehyde $\tilde{A}-\tilde{X}$ $2_0^2 4_0^1$ vibronic band, acquired with 700 mTorr formaldehyde. Panel (a) shows the measured data while (b) shows a spectral simulation of the corresponding region, where red lines indicate line positions and relative intensities and the black line is a prediction of the spectrum with Doppler line widths. Asterisks represent features used for peak absorption cross-section measurements as described in the text.

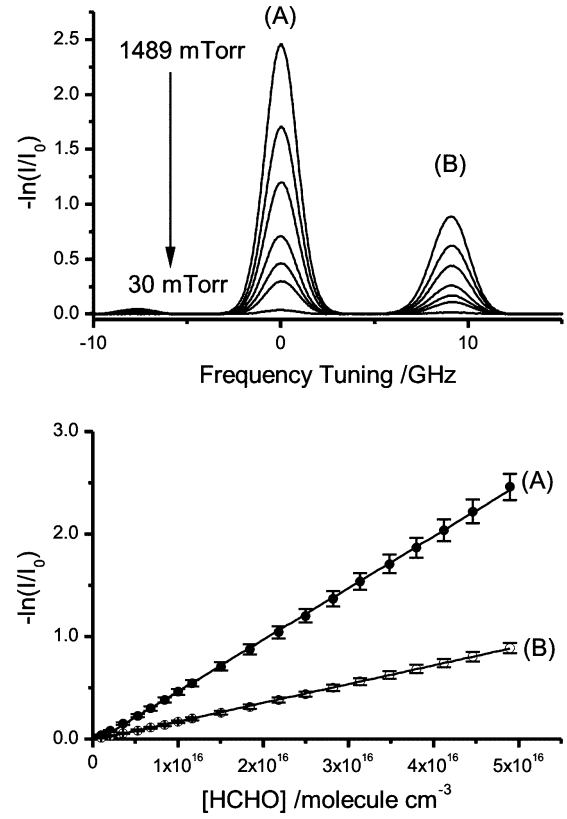

Figure 4. Example data used for peak absorption cross-section measurements. The top panel shows a selection of absorption spectra, centered on the $^{p}Q_{7,1}(8)$ line (marked A) at 30635.31 cm^{-1}, recorded at pressures ranging between 30 and 1489 mTorr. Peak (B) is a feature comprising the overlapped lines $^{p}R_{20,1}(20)$, $^{r}R_{13,2}(14)$, and $^{p}R_{7,2}(9)$ centered at 30635.58 cm^{-1}. The bottom panel shows plots of peak absorbance against pressure for the two absorption features as marked, along with the best linear fits used to calculate the absorption cross sections, as given in Table 1.

We can also make a comparison with the data of Motsch et al.,[16] who probed the entire $2_0^2 4_0^1$ band with an instrumental resolution of around 1.67×10^{-5} cm^{-1}. In regions where our spectra overlap with theirs, we find excellent agreement; the relative positions and intensities of equivalent features are essentially identical, allowing for differences resulting from the different formaldehyde pressures used. This is expected, as in each case the apparent resolution is limited by the Doppler width of the spectral features. Comparison with the data of Motsch et al. also confirms the presence of an absorption feature on the left of Figure 2a that does not appear in the simulation. As mentioned earlier, we have not attempted to perform any further optimization of the spectroscopic constants by fitting to our data, but the fact that the line appears in both sets of independently measured data suggests that it is real and not an artifact, for example, of an undetected mode hop of our laser source.

It is worth noting that the widths of the spectral features in Figures 2 and 3 show good agreement with the predicted full width half-maximum (fwhm) thermal Doppler width of 2.06 GHz, or 0.069 cm^{-1}. For further verification, spectra of isolated rotational lines were recorded at lower pressures (10−50 mTorr) of formaldehyde, where the line shape should be dominated by Doppler broadening and self-pressure broadening effects should be minimal. Gaussian functions fitted to these profiles return widths that agree with the predicted width within an uncertainty of ±3%, indicating that there is no significant contribution to the line shape from lifetime broadening. This is not necessarily surprising, as the $2_0^2 4_0^1$ band lies below the threshold where excitation to the upper (S_1) state is followed by rapid intersystem crossing to unbound levels in the T_1 state, resulting in dissociation to the radical products H + HCO*.[22] Dissociation to H + HCO can also occur via nonradiative transfer to high lying unbound levels in the ground (S_0) state without a potential barrier or by crossing to lower lying levels in the T_1 state, resulting in H_2 + CO via a potential barrier. Our results are consistent with previous studies of formaldehyde photochemistry,[23,24] which demonstrate that these processes shorten the lifetimes of the S_1 state rovibronic levels probed in this work to around 10 ns. This would add approximately 15 MHz to the line width, which is within the uncertainty limits of our frequency scale determination. We intend, in future work, to probe regions of the $\tilde{A}-\tilde{X}$ band system at shorter wavelengths and with greater vibronic excitation, in order to study predissociation rates.

Absorption Cross Sections. In addition to the contiguous absorption spectra shown in Figures 2 and 3, we have performed absolute peak absorption cross-section measurements using several isolated rotational lines spread across a ~120 cm^{-1} range in the $2_0^2 4_0^1$ band. This was achieved by tuning the UV source to the selected line and measuring absorption spectra as a function of increasing formaldehyde pressure. Figure 4 shows an example, where the top panel displays a series of spectra measured over a range of pressures, containing a single rotational line (labeled A), assigned[13,19] in the notation $^{\Delta K_a}\Delta N_{K_c K_a}(J)$ as $^{p}Q_{7,1}(8)$ at 30635.31 cm^{-1}. Also shown is a blended feature (B) containing the three overlapping lines $^{p}R_{20,1}(20)$, $^{r}R_{13,2}(14)$, and $^{p}R_{7,2}(9)$ centered at 30635.58 cm^{-1},

TABLE 1: Measured Absolute Peak Absorption Cross Sections of a Selection of Formaldehyde Lines in the $\tilde{A}-\tilde{X}$ $2_0^2 4_0^1$ Band

assignment[a]	wavenumber /cm^{-1}	σ /$\times 10^{-19}$ cm^2 molecule^{-1}	
		this work	PGopher[b]
$^pQ_{9,5}(14)/^pQ_{10,5}(14)$	30540.28	3.15 ± 0.17	2.81
$^pQ_{12,2}(13)$	30598.20	1.09 ± 0.06	1.07
$^rR_{23,3}(26)$	30634.98	0.18 ± 0.01	0.16
$^pQ_{7,1}(8)$	30635.31	10.1 ± 0.51	8.87
$^pR_{20,1}(20)/^pR_{13,2}(14)/^pR_{7,2}(9)$	30635.58	3.65 ± 0.18	3.39
$^rQ_{12,1}(13)$	30644.82	5.46 ± 0.29	5.36
$^rQ_{4,5}(8)/^rQ_{3,5}(8)$	30715.06	2.29 ± 0.12	2.32
$^rR_{11,5}(16)/^rR_{12,5}(16)$	30716.44	2.10 ± 0.11	2.07

[a] Using the notation $^{\Delta K_a}\Delta N_{K_c K_a}(J)$. [b] Values predicted by PGopher,[19] using the transition moment data of Smith et al.[13]

along with a much weaker line, $^rR_{23,3}(26)$ at 30634.98 cm^{-1}, on the left-hand side of the spectrum. Despite its weak intensity, this third feature still has a sufficient signal/noise ratio for use in a cross-section measurement. As before, the intensity scale is plotted as the base e absorbance, $-\ln(I/I_0)$. The bottom panel of the figure shows a plot of the peak absorbance against concentration of formaldehyde for the two stronger absorption features, in units of molecules cm^{-3}. From eq 1 the peak absorption cross sections can be easily extracted from the slope of these plots, by accounting for the path length of 50 cm.

The full set of measured cross sections is given in Table 1 and is markedly larger than those recorded in the literature,[10−14] where instrumental broadening was significant. A more direct comparison is to the cross sections predicted by PGopher, again using the input parameters supplied by Smith et al.[13] These include an optimized value for the transition dipole moment of the $2_0^2 4_0^1$ band which, after their instrumental bandwidth was accounted for by fitting to rotational fine structure, resulted in the best agreement with their experimentally measured cross sections. As before, we have simply changed the resolution function to match the Doppler widths of the spectral features. This results in good agreement, with the deviation between our measured values and the simulations typically varying between ~1 and 13%, which is in many cases somewhat larger than our uncertainty limits. While the purity of the formaldehyde samples used across all of our individual measurements is likely to be a source of the change in the deviation, in nearly all cases we measure a cross section *greater* than that predicted, suggesting that sample purity is not the sole cause of the discrepancy. A small increase in the transition moment from 0.032 to 0.033 D produces better agreement within our range of measured cross sections; however we would be hesitant to recommend the change as an improvement without a larger selection of data to compare.

Pressure Broadening. To investigate the effects of buffer gas pressure on the observed line shape, the spectrometer was tuned to scan over the line $^rQ_{12,1}(13)$ at 30644.82 cm^{-1}. Spectra were then recorded with a fixed pressure of formaldehyde, typically in the range 200−800 mTorr, in the presence of a range of pressures of the chosen buffer gas, including CO_2, N_2, O_2, and a selection of noble gases. Self-broadening was also investigated, by recording spectra with varying pressures of pure formaldehyde. In this case, a smaller cell with a path length of 5 cm was used to allow a greater range of pressures to be used while remaining in the linear absorption regime. The experiments were then repeated using another rotational feature, assigned as $^rQ_{4,5}(8)/^rQ_{3,5}(8)$ at 30715.06 cm^{-1}. Figure 5a shows an example of the measured spectra, with the initial sample of pure formaldehyde plotted as squares, and spectra recorded following addition of 200 and 400 Torr of N_2 plotted as circles and triangles, respectively.

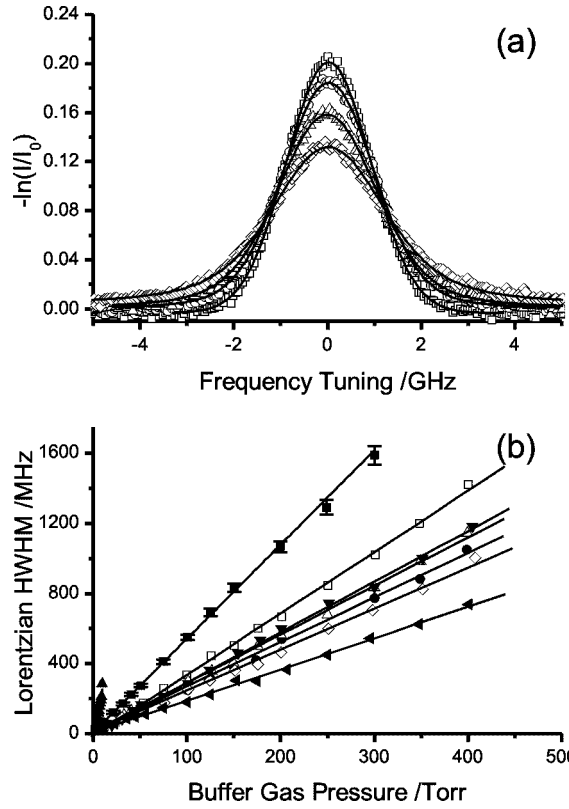

Figure 5. Example data used for the calculation of pressure broadening coefficients. The top panel shows absorption spectra of the $^rQ_{12,1}(13)$ line at 30644.82 cm^{-1}, acquired with 220 mTorr formaldehyde in the presence of: (open box) no buffer gas, (open circle) 75 Torr O_2, (open triangle) 150 Torr O_2 and (open diamond shape) 250 Torr O_2. Solid lines are best fit Voigt profiles with the Gaussian width fixed at 2.06 GHz and returned Lorentzian half width values of 0.01 ± 0.01, 0.22 ± 0.01, 0.40 ± 0.01, and 0.68 ± 0.01 GHz, respectively. The bottom panel shows plots of the extracted Lorentzian half-width against pressure for self-broadening (solid triangle up), and the buffer gases CO_2 (solid box), N_2 (open box), He (solid triangle down), O_2 (open triangle up), Ar (solid circle), Kr (open diamond shape), and Ne (solid triangle left) along with the best linear fits used to calculate the broadening parameter, γ. For clarity, representative error bars are shown for the CO_2 data only.

As mentioned earlier, the line shape in the absence of pressure broadening is described by a Gaussian function, due to Doppler broadening. Pressure broadening adds a Lorentzian component, resulting in an overall line shape described by a Voigt function. To characterize the pressure broadening process, a Voigt function was fitted to the line shape recorded at each pressure for each buffer gas. The Gaussian width of the fit was fixed at the known Doppler width and the Lorentzian width allowed to vary to achieve the best fit. The linear variation of the returned Lorentzian width of the $^rQ_{12,1}(13)$ line with pressure is plotted

TABLE 2: Measured Pressure Broadening Parameters

broadening species	γ /MHz Torr^{-1}	
	$^rQ_{4,5}(8)/^rQ_{3,5}(8)$	$^rQ_{12,1}(13)$
CH_2O	20.0 ± 0.49	28.8 ± 0.33
CO_2	5.04 ± 0.18	5.25 ± 0.13
N_2	3.63 ± 0.12	3.56 ± 0.10
O_2	2.69 ± 0.06	2.79 ± 0.04
Kr	2.38 ± 0.02	2.35 ± 0.02
Ar	2.41 ± 0.10	2.36 ± 0.18
Ne	1.78 ± 0.02	1.77 ± 0.02
He	2.34 ± 0.01	2.71 ± 0.24

in Figure 5b for the range of buffer gases and gives the broadening parameter γ as the slope in each case, quoted as the half width at half-maximum (hwhm) in units of MHz Torr^{-1}. The resulting broadening parameters for each gas are listed in Table 2.

To our knowledge there are no pressure broadening studies of equivalent formaldehyde transitions in the literature with which we can make a direct, quantitative comparison to our data. There are however a few examples where we can make qualitative comparisons. Co et al.[14] determined a coefficient for air broadening of 5.3 MHz Torr^{-1} by fitting Voigt profiles to selected lines in the $2_0^0 4_0^1$ band, recorded in the presence of varying pressures of dry air. A weighted sum of our coefficients according to the atmospheric mixing ratio shows only fair agreement with this value, at 3.46 MHz Torr^{-1}. It is worth noting however that Co et al. did not state whether their value was fwhm or hwhm, so the agreement may be better than that described above, depending on their definition of the parameter γ. The most comprehensive pressure broadening studies that we are aware of have been carried out with multiple collision partners in the near-infrared region on selected rotational lines in the $2\nu_5$ vibrational overtone band,[25] on two rotational lines in combination bands around 6700 cm^{-1},[26] and in the far-infrared[27] on a single rotational line of the ν_1 fundamental band. Our experiments obviously probe a very different upper state to the previous work, so we would not necessarily expect to measure very similar values in comparison to these earlier studies. Our values are typically lower than those measured in the infrared regions and beyond by up to ~20%. This is consistent with the fact that the dipole moment of the $^1A_2$ state[28] is markedly reduced to 1.56 D, compared with 2.33 D in the ground electronic state.[29] A component of our measurements therefore probes the weaker interaction between electronically excited formaldehyde and the broadening gas, resulting in the observed reduction in broadening efficiency.

The expected trend that the broadening parameter scales with the strength of the intermolecular interaction between formaldehyde and the collision partner is clearly seen in our data. Self-broadening is considerably more efficient than broadening by any of the buffer gases due to the strong dipole−dipole interaction between formaldehyde molecules and the possibility of resonant collisional energy transfer. Broadening by the three molecular buffer gases is governed by a dipole−quadrupole interaction and scales in the order $CO_2 > N_2 > O_2$, with the strength of their quadrupole moments.[30] With the noble gases, the broadening interaction is mediated by weaker Van der Waals forces and should scale across the range with the magnitude of their polarizability. This can be quantified by using the Parmenter−Seaver model,[31] which relates the efficiency of a collisional process to the depth of the intermolecular potential well between the colliding species Q and M, ε_{QM}. The quantity ε_{QM} is unknown for our range of formaldehyde−noble gas interactions but is often approximated[31] to the geometric average of the well depths between pairs of each colliding species, given by eq 2

$$\varepsilon_{QM} = \sqrt{\varepsilon_{QQ}\varepsilon_{MM}} \tag{2}$$

The intermolecular well depth between pairs of formaldehyde molecules is a common factor among the range of experiments, so eq 2 can be further reduced to include only the well depth between pairs of noble gas atoms, ε_{MM}. The Parmenter−Seaver relationship is then given by eq 3

$$\ln \sigma = \ln C + \beta\left(\frac{\varepsilon_{MM}}{k}\right)^{1/2} \tag{3}$$

where C is a collection of empirical constants, k is Boltzmann's constant, and σ is in our case the pressure broadening coefficient expressed as a collision cross section. This is done by conversion of the broadening parameter to units of Hz Pa^{-1}, followed by multiplication by the factor $2\pi kT/\upsilon_{rel}$, where υ_{rel} is the mean relative velocity of the formaldehyde-broadening partner pair.[25] Variations in the collision rate due to the relative masses of the collision partners are thus accounted for. If eq 2 holds, then the parameter β depends upon the intermolecular well depth between formaldehyde monomers, as shown in eq 4 below.

$$\beta = \sqrt{\frac{\varepsilon_{QQ}}{kT^2}} \tag{4}$$

Figure 6 shows an example Parmenter−Seaver plot using broadening parameters recorded on the $^rQ_{12,1}(13)$ rotational line. The figure shows a good correlation between broadening efficiency and ε_{MM} for the noble gases, which adhere to a linear trend as predicted by eq 3. The slope suggests a value for the well depth between pairs of formaldehyde molecules of 5.33 ± 0.26 kJ mol^{-1}. This analysis assumes that the approximation given in eq 2 is correct; however on closer inspection this does not appear to be true in this case. Ab initio calculations of the formaldehyde dimer[32] predict two isomers, with the average well depth (D_e) to be 11.2 kJ mol^{-1}. Using this value in eq 2 along with the corresponding D_e value for the Ar dimer[33] of 1.2 kJ mol^{-1}, a formaldehyde−Ar well depth of 3.6 kJ mol^{-1} is predicted, which is considerably larger than that suggested by theoretical studies, 2.0 kJ mol^{-1}.[34] This comparison would in principle be more relevant using D_0 energies, but we are not aware of any experimental or theoretical D_0 values for the formaldehyde−argon complex. Substitution of D_0 energies[32,33] for the formaldehyde and argon dimers into eq 2 results in an implied formaldehyde−argon well depth of 2.4 kJ mol^{-1}, which exceeds the known D_e value by some 0.4 kJ mol^{-1} and is thus unlikely to be accurate. The breakdown of the approximation is likely due to the difference in the binding intermolecular forces between the formaldehyde dimer and the formaldehyde−argon complex and suggests caution against the use of the absolute value of the slope of eq 3 in a quantitative determination of the binding energy for this system. It is however interesting to note that the value we record from the slope is lower than that inferred by the same method from measurements in the near-infrared region,[25] which is 9.40 ± 0.14 kJ mol^{-1}. As described earlier, we should expect such a parameter to be reduced in our measurement, due to the smaller upper state dipole moment.

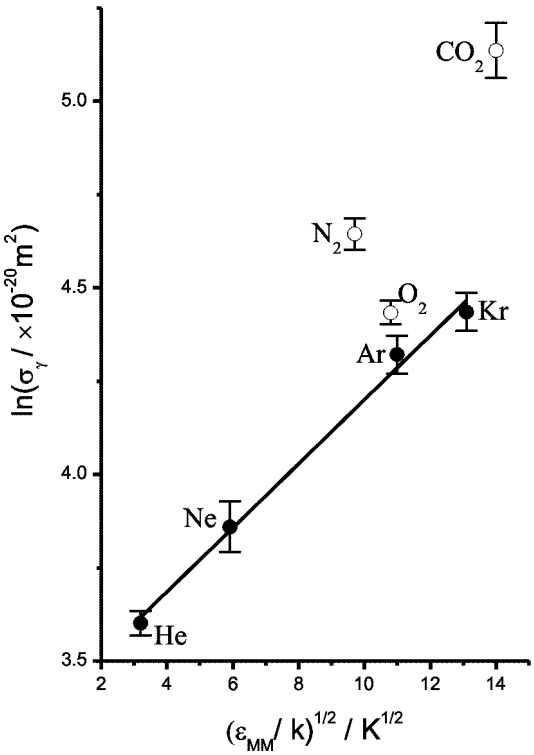

Figure 6. Plot of the Parmenter−Seaver correlation between intermolecular well-depth of the buffer gases (●) He, Ne, Ar, and Kr with observed broadening parameter, expressed as a cross section. The linear fit suggests a value for the well depth between formaldehyde monomers, as described in the text, of 5.33 ± 0.26 kJ mol^{-1}. Also shown for comparison, but not included in the fit are the molecular collision partners (○) CO_2, N_2, and O_2.

Cavity-Enhanced Absorption Spectroscopy. To enhance the sensitivity of the spectrometer, a pair of high reflectivity mirrors was installed inside the absorption cell, to form an optical cavity in order to utilize the cavity enhanced absorption methodology. The absorbance in this case is described by the following eq 5[35]

$$\frac{I_0(\nu) - I(\nu)}{I(\nu)} = \frac{\sigma(\nu)cl}{1 - R} \qquad (5)$$

where $I_0(\nu)$ and $I(\nu)$ are the measured intensity in the absence and presence of formaldehyde, respectively, $\sigma(\nu)$ is the absorption cross section, and c is the concentration. The physical separation of the cavity mirrors is given by l, which was equal to 45.7 cm in the experiments, while R is the geometric mean of the mirror reflectivities, in this case stated by the manufacturer to be 0.999. We would therefore expect a path length enhancement factor of approximately 3 orders of magnitude, compared to direct absorption. This increased sensitivity required the use of a permeation tube formaldehyde source, as described in the Experimental Section, to provide a mixture containing a specified concentration of formaldehyde which was low enough to allow measurements to be recorded accurately.

Figure 7 shows an example spectrum, recorded with the optical cavity in place, featuring the same region as illustrated for direct absorption in Figure 4, containing the $^{p}Q_{7,1}(8)$ line. Cavity-enhanced absorption is an absolute technique, if the reflectivity of the cavity mirrors is known accurately. A measurement of the reflectivity, typically achieved by ring down[36] or phase shift[37] techniques, would therefore allow an absolute concentration measurement to be made using the relevant cross sections from Table 1 and compared to that predicted by the permeation source calibration. However, such a measurement is challenging where low light intensities are coupled into the cavity, as in this case, and a detector with sufficient time response *and* sensitivity was not available to us.

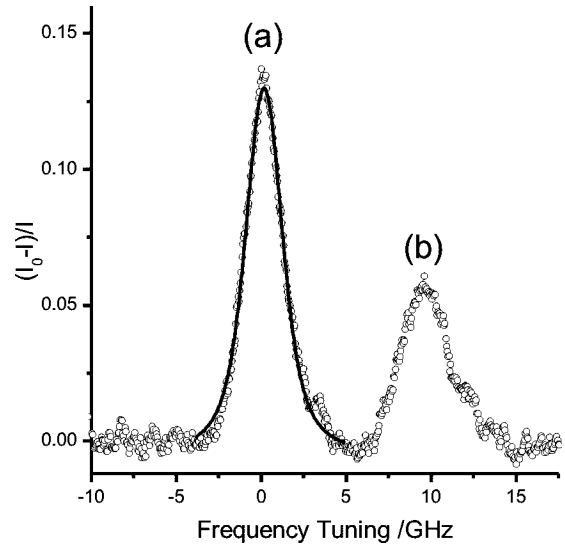

Figure 7. Example data from the cavity-enhanced absorption experiment, showing a spectrum containing (a) the $^{p}Q_{7,1}(8)$ line and (b) a blended feature consisting of $^{p}R_{20,1}(20)$, $^{p}R_{13,2}(14)$, and $^{p}R_{7,2}(9)$, recorded in the presence of a mixture of 2.9 ppmv formaldehyde in 154.5 Torr N_2, corresponding to a CH_2O number density of 1.5×10^{13} molecules cm^{-3}. The solid line is a Voigt fit to the spectral feature of interest, for illustrative purposes. The associated α_{min} is 1.2×10^{-6} cm^{-1} Hz$^{-1/2}$, which indicates a minimum detectable concentration at atmospheric pressure of 172 ppbv Hz$^{-1/2}$.

As an alternative approach, we compared the measured absorbance of a particular absorption feature, such as that shown in Figure 7, with the corresponding concentration predicted by the permeation source calibration and our known absorption cross section. Substitution of these parameters into eq 5, along with the physical cavity length then allows calculation of the mirror reflectivity, assuming that the permeation source calibration is correct. We repeated this process using sample mixtures with concentrations ranging between 2.9 and 4.6 ppmv. Our reflectivity values ranged between 0.996 and 0.997 over a period of several weeks, the exact value depending on precise alignment of the system. In all cases, the appropriate measured value for the experimental conditions was applied during analysis of the data.

For further verification, we acquired spectra of the $^{r}R_{23,3}(26)$ line using samples of formaldehyde prepared by the cracking of paraformaldehyde, as used in the direct absorption measurements. This line is sufficiently weak to allow moderate pressures (50−200 mTorr) of formaldehyde to be probed accurately by cavity-enhanced absorption and is located within ∼0.3 cm^{-1} of the $^{p}Q_{7,1}(8)$ line, meaning that variation in the reflectivity with wavelength between the two features will not be significant. We can then compare the measured absorbance with our measured absorption cross section for this line, given in Table 1, to allow a determination of the mirror reflectivity and thus check for consistency with the expected concentrations provided by the permeation source. By this method we calculate a reflectivity of 0.997, which is in excellent agreement with the reflectivity calculated from measurements with the permeation source.

There is a clear increase in the noise level for the CEAS data, as expected due to the much lower signal levels, and the presence of unwanted residual mode noise as a direct consequence of the cavity. The level of noise in the data shown in Figure 7 of the $^{p}Q_{7,1}(8)$ line, recorded by averaging 1024 scans acquired over approximately 40 s, corresponds to an acquisition time reduced noise equivalent absorption, α_{min}, of 1.2×10^{-6} cm^{-1} Hz$^{-1/2}$, which is lower than sensitivities commonly achieved[35,38,39] using this technique but reasonable given the low laser intensity coupled into the cavity. The noise level used in this calculation was obtained from the standard deviation of a linear fit to the ~5 GHz range of baseline to the left of feature (a) in the figure. This corresponds to approximately twice the fwhm of the pressure broadened spectral feature of interest. Allan variance analysis[40] suggests that further signal averaging beyond ~45 s in our case does not significantly improve the sensitivity.

From a combination of our measured N_2 and O_2 pressure broadening coefficients we predict that the peak absorption cross section of the $^{p}Q_{7,1}(8)$ line would be reduced to 3.3×10^{-19} cm^2 molecule^{-1} in air at atmospheric pressure. Noise equivalent absorption would therefore correspond to a number density detection limit of 3.9×10^{12} molecules cm^{-3} Hz$^{-1/2}$ or, expressed as an atmospheric pressure value, 160 ppbv Hz$^{-1/2}$. We estimate that Rayleigh scattering would reduce the sensitivity by around a further 8%, based on an extrapolation of measured scattering cross sections,[41] leading to a value of 172 ppbv Hz$^{-1/2}$. This value is somewhat higher than the World Health Organization recommended exposure limit of 80 ppbv[42] and typical ground level concentrations of up to 20 ppbv in polluted urban environments. The sensitivity could in principle be improved by selecting a stronger absorption feature. Although the line we selected is among the strongest in the $2_0^2 4_0^1$ vibronic band, blended absorption features are present in other regions of the band which could offer improvements of around 20%. Further enhancements in sensitivity could be made by improving the power output of the system, for example, by performing the frequency up-conversion in a resonant optical cavity or by potentially using frequency doubling in periodically poled or waveguide materials. This would allow the use of higher reflectivity cavity mirrors in the absorption cell, thus providing greater path length enhancement, as well as the possibility of applying the more sensitive cavity ring down spectroscopy (CRDS) technique.

Conclusions

We have constructed a narrow bandwidth UV absorption spectrometer by sum-frequency mixing of a near-infrared diode laser with a visible diode pumped solid-state laser in β-BBO. The instrument has been used to measure absolute absorption cross sections and pressure broadening coefficients of selected rotational lines in the $\tilde{A}-\tilde{X}$ $2_0^2 4_0^1$ vibronic band of formaldehyde around 326 nm. Our measured absorption cross sections were found to be considerably larger than those found in the literature, where instrumental broadening was comparable to, or larger than, the Doppler width, but in good agreement with those predicted by best fit spectral simulations of Smith et al.[13] Pressure broadening coefficients have been determined for two rotational lines with a range of buffer gases, and show a weaker broadening propensity compared to measurements carried out in the infrared regions. This is expected due to the reduced dipole moment of the upper state probed in this work. The sensitivity of the instrument was enhanced by the incorporation of an optical cavity and the potential for atmospheric monitoring explored. A detection limit of 172 ppbv Hz$^{-1/2}$ in atmospheric air is achievable with the current setup.

Acknowledgment. We thank EPSRC (RLV CP1E019765/1) and The Leverhulme Trust (F/08 788/E) for funding. Studentships for S.R.T. and M.B.C. were provided by DIAC and NERC, respectively. G.A.D.R. thanks the Royal Society for funding. We also thank Professor Andrew Orr-Ewing for the generous loan of the cavity mirrors used in this work and Dr. Colin Western for his valuable advice regarding the PGopher simulations.

References and Notes

(1) Williams, I. D.; Revitt, D. M.; Hamilton, R. S. *Sci. Total Environ.* **1996**, *189/190*, 475.
(2) Viskari, E.-L.; Vartiainen, M.; Pasanen, P. *Atmos. Environ.* **2000**, *34*, 917.
(3) Wang, B.; Lee, S. C.; Ho, K. F. *Atmos. Environ.* **2007**, *41*, 2851.
(4) Lowe, D. C.; Schmidt, U. *J. Geophys. Res.* **1983**, *88*, 10844.
(5) Hutterli, M. A.; McConnel, J. R.; Chen, G.; Bales, R. C.; Davis, D. D.; Lenschow, D. H. *Atmos. Environ.* **2004**, *38*, 5439.
(6) Moule, D. C.; Walsh, A. D. *Chem. Rev.* **1975**, *75*, 67.
(7) Clouthier, D. J.; Ramsay, D. A. *Annu. Rev. Phys. Chem.* **1983**, *34*, 31.
(8) Gratien, A.; Nilsson, E.; Doussin, J.-F.; Johnson, M. S.; Nielsen, C. J.; Stenstrom, Y.; Picquet-Varrault, B. *J. Phys. Chem. A* **2007**, *111*, 11506.
(9) Barry, H. R.; Corner, L.; Hancock, G.; Peverall, R.; Ritchie, G. A. D. *Phys. Chem. Chem. Phys.* **2002**, *4*, 445.
(10) Cantrell, C. A.; Davidson, J. A.; McDaniel, A. H.; Shetter, R. E.; Calvert, J. G. *J. Phys. Chem.* **1990**, *94*, 3902.
(11) Meller, R.; Moortgat, G. K. *J. Geophys. Res.* **2000**, *D105*, 7089.
(12) Pope, F. D.; Smith, C. A.; Ashfold, M. N. R.; Orr-Ewing, A. J. *Phys. Chem. Chem. Phys.* **2005**, *7*, 79.
(13) Smith, C. A.; Pope, F. D.; Cronin, B.; Parkes, C. B.; Orr-Ewing, A. J. *J. Phys. Chem. A* **2006**, *110*, 11645.
(14) Co, D. T.; Hanisco, T. F.; Anderson, J. G.; Keutsch, F. N. *J. Phys. Chem. A* **2005**, *109*, 10675.
(15) Gratien, A.; Picquet-Varrault, B.; Orphal, J.; Perraudin, E.; Doussin, J.-F.; Flaud, J.-M. *J. Geophys. Res.* **2007**, *112*, D05035.
(16) Motsch, M.; Schenk, M.; Zeppenfeld, M.; Schmitt, M.; Meerts, W. L.; Pinkse, P. W. H.; Rempe, G. *J. Mol. Spectrosc.* **2008**, *252*, 25.
(17) Boyd, G. D.; Kleinman, D. A. *J. Appl. Phys.* **1968**, *39*, 3597.
(18) Spence, R.; Wild, W. *J. Chem. Soc.* **1935**, *1*, 338.
(19) Western, C. M. *PGopher, a program for simulating rotational structure*. University of Bristol, http://pgopher.chm.bris.ac.uk.
(20) Brand, J. C. D.; Stevens, C. G. *J. Chem. Phys.* **1973**, *58*, 3331.
(21) Birss, F. W.; Ramsay, D. A.; Till, S. M. *Chem. Phys. Lett.* **1978**, *53*, 14.
(22) Yin, H. M.; Kable, S. H.; Zhang, X.; Bowman, J. M. *Science* **2006**, *311*, 1443.
(23) Selzle, H. L.; Schlag, E. W. *Chem. Phys.* **1979**, *43*, 111.
(24) Miller, R. G.; Lee, E. K. C. *J. Chem. Phys.* **1978**, *68*, 4448.
(25) Barry, H. R.; Corner, L.; Hancock, G.; Peverall, R.; Ranson, T. L.; Ritchie, G. A. D. *Phys. Chem. Chem. Phys.* **2003**, *5*, 3106.
(26) Staak, M.; Gash, E. W.; Venables, D. S.; Ruth, A. A. *J. Mol. Spectrosc.* **2005**, *229*, 115.
(27) Burkart, M.; Schramm, B. *J. Mol. Spectrosc.* **2003**, *217*, 153.
(28) Freeman, D. E.; Klemperer, W. *J. Chem. Phys.* **1966**, *45*, 52.
(29) Fabricant, B.; Krieger, D.; Muenter, J. S. *J. Chem. Phys.* **1977**, *67*, 1576.
(30) Stogryn, D. E.; Stogryn, A. P. *Mol. Phys.* **1966**, *11*, 371.
(31) Lin, H.-M.; Seaver, M.; Tang, K. Y.; Knight, A. E. W.; Parmenter, C. S. *J. Chem. Phys.* **1979**, *70*, 5442.
(32) Vila, A.; Graña, A. M.; Mosquera, R. A. *Chem. Phys.* **2002**, *281*, 11.
(33) Le Roy, R. J. *J. Chem. Phys.* **1972**, *57*, 573.
(34) Sadlej, J.; Szczęśniak, M. M.; Chałasiński, G. *J. Chem. Phys.* **1993**, *99*, 5211.
(35) Berden, G.; Peeters, R.; Meijer, G. *Int. Rev. Phys. Chem.* **2000**, *19*, 565.
(36) Scherer, J. J.; Paul, J. B.; O'Keefe, A.; Saykally, R. J. *Chem. Rev.* **1997**, *97*, 25.
(37) Herbelin, J. M.; McKay, J. A.; Kwok, M. A.; Ueunten, R. H.; Urevig, D. D.; Spencer, D. J.; Benard, D. J. *Appl. Opt.* **1980**, *19*, 144.
(38) Bakowski, B.; Corner, L.; Hancock, G.; Kotchie, R.; Peverall, R.; Ritchie, G. A. D. *Appl. Phys. B: Laser Opt.* **2002**, *75*, 745.
(39) Mazurenka, M.; Orr-Ewing, A. J.; Peverall, R.; Ritchie, G. A. D. *Annu. Rep. Prog. Chem., Sect. C* **2005**, *101*, 100.
(40) Allan, D. W. *Proc. IEEE* **1966**, *54*, 221.
(41) Ityaksov, D.; Linnartz, H.; Ubachs, W. *Mol. Phys.* **2008**, *106*, 2471.
(42) *Air Quality Guidelines for Europe*, 2nd ed.; WHO Regional Publications, European Series No. 91; World Health Organization Regional Office for Europe: Copenhagen, 2000; p 87.

JP9023475